ET Enterprises electron tubes

technical reprint

R/P098

fast timing with slow scintillators

fast timing with slow scintillators

A G Wright, Electron Tubes Ltd., Bury Street, Ruislip, HA4 7TA, UK

technical reprint R/P098

1 introduction

This study concerns timing with slow, inorganic scintillators; particularly where the emission involves few photons. Monte Carlo simulations are used to mimic the statistical nature of both the light emission and the photomultiplier (pmt) behaviour. Simulated waveforms highlight practical difficulties concerning multiple triggering. Important pmt attributes are discussed.

This topic was extensively studied fifty years ago following the seminal paper by Post and Shiff[1] which set an upper limit to timing fidelity. Gatti[2] and his co-workers allowed for pmt parameters, such as single electron response (SER) and transit time jitter. Although analytic solutions can sometimes be found, most authors ultimately resort to Monte Carlo simulations, and this approach has been adopted in the present work. Early work ($\tau \sim 1ns$) concerned fast plastic scintillators but currently there is growing interest in timing with high Z, slow scintillators ($\tau \sim 500$ ns). These are listed in **table 1** together with the relatively new, high Z, scintillators. The intention in this paper is to understand how pmt parameters affect timing with slow scintillators, especially where photon numbers are low.

Consideration is given to Constant Fraction (CF) discrimination.

2 time distribution of photons

Restricting ourselves to small volume scintillators, the light output from 0 to t may be taken as

$$Q(t) = R(1- e^{-t/\tau}) \quad \text{... (1)}$$

where R is the total number of photons in the pulse. (1) is plotted in **figure 1** together with a simulation showing how an actual event follows a random walk.

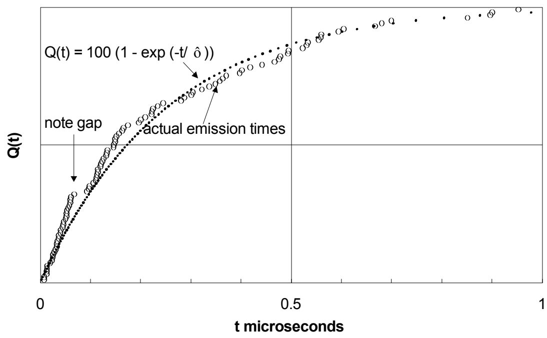

figure 1 the random nature of photon emission from a scintillator - the accentuated time gaps are of particular concern.

table 1

timing characteristics. ρ is the density g/cm^3 and *ph/keV* is the photon yield per keV

scintillator	ρ	τ, ns	ph/keV	R/τ(FOM)
BC418	1.03	1.4	8	5.7
BC400	1.03	2.4	8	3.3
$LaCl_3$	3.79	28	49	1.8
LuAP	8.30	18	20	1.1
YAP(Ce)	5.55	28	7	0.25
NaI(Tl)	3.67	250	40	0.16
CsI(Tl)	4.51	1000	60	0.06
BGO	7.13	300	8	0.03
$CdWO_4$	8.00	5000	14	0.003

The probability distribution, $P(t)$, for the arrival of the Qth photon, at a time between t and t + dt is given by [1] and [3], where R is taken as the mean of a Poisson distribution $p(n) = R^n e^{-R}/n!$

$$P(t) = R^Q \exp(-R(1-e^{-t/\tau}))(1-e^{-t/\tau})^{Q-1} e^{-t/\tau} dt \quad \text{...(2)}$$

Timing distributions for various values of Q are plotted in **figure 2** for $R = 100$ and $\tau = 250$ ns.

The variance of P is given in [1], subject to $R >> 1$ and $R >> Q$, as

$$var(Q) = Q\,(\tau/R)^2\,(1 + 2(1+Q)/R + ...) \quad \text{...(3)}$$

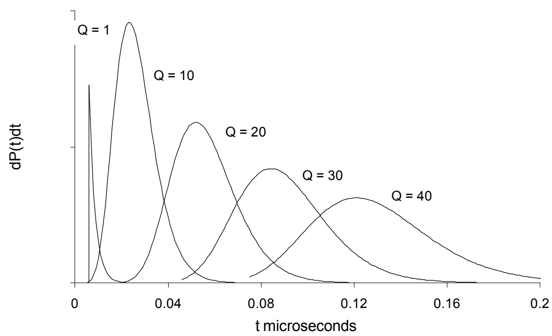

figure 2 timing distributions for the arrival of the Qth photon out of R. Best timing is obtained with Q = 1, where P(t) ~ R/τ exp(-(R+1)τ/t).

Otherwise the variance must be calculated from the curves of **figure 2**. Equation 3 suggest a Figure of merit $(FOM) = R/\tau$ for $\sigma(Q)$, the standard deviation. **Table 1** lists a range of scintillators and their major properties of interest.

So far we have considered the statistics of light emission from a scintillator. Considering the pmt the foregoing treatment, however, applies equally to photoelectron emission and we need only take the quantum efficiency into account.

3 effect of pmt parameters

3.1 transit time dispersion, ε_{ph}

Simulations were run to select photoemission times in accordance with (1). The time dispersion of the multiplier was mimicked by randomising the arrival time of each pulse at the anode in accordance with a normal distribution, characterised by (μ, ε_{ph}), where μ is the mean transit time and ε_{ph} is its standard deviation. The arrival times at the anode were then ordered to provide the time signature of an R-photoelectron event. This was repeated many times yielding a distribution from which to calculate σ(Q). The results shown in **figure 3** illustrate that pmt jitter is not significant where photon-poor signals are concerned, whereas for R = 5000 (~500 keV in NaI(Tl)), for example, the timing is dominated by the pmt performance.

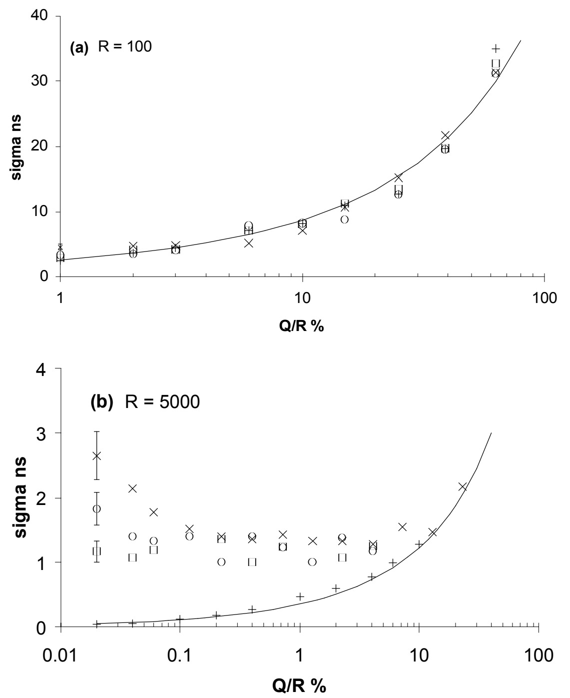

figure 3. $\sigma(Q)$ determined directly from (2),+, compared with (3), solid line. $R = 100$ and 5000 for (a) and (b) respectively. The marked effect of pmt jitter is evident in (b) where it dictates the performance for $Q/R < 10\%$. The sporadic error bars give an indication of the precision of the simulations. □: $\varepsilon_{ph} = 1$ ns; O: $= 2.5$ ns; $x = 5$ ns

3.2 noisy gain, (noise factor = NF)

The single electron response (SER) of a pmt is the pulse height distribution for anode signals initiated by single photons. A noiseless multiplier is characterised by a δ-function response, such as (a) in **figure 4**. Plot (b) illustrates a 'good' SER, showing a peak in the distribution, whereas curve (c) shows a noisy multiplier with an exponential-like distribution. We define a noise factor, $NF = [1+ \varepsilon_A]^{1/2}$, where $\varepsilon_A = var(h)/<h>^2$, is the gain dispersion, calculated directly from the SERs shown in **figure 4**.

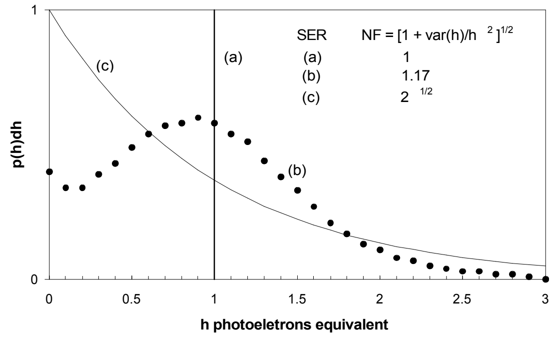

figure 4 pmt single electron response curves, SER.(a) noiseless gain (b) a 'good' SER and (c) a poor SER.

4 the signal forming process at the anode

We assume a characteristic anode pulse shape, i(t), prescribed for every photoelectron-initiated event. If $q = e<g>$ then $i(t) = q/\tau_s \exp(-t/\tau_s)$ where τ_s is the characteristic width of the anode pulse. More complicated forms may be assumed for i(t) but the above is sufficient. The signal at the anode, describing the entire scintillation event is given by convolution.

$$I(t) = Q'(t) \otimes i(t)$$
$$= Rq/(t - \tau_s)\,[\exp(-t/\tau) - \exp(-t/\tau_s)] \quad ...(4)$$

We can derive an expression for the voltage signal across an anode load of $R' // C'$ from (4), thus

$$v_0(t) = R'qR\tau / [(\tau - \tau_s)(\tau_0 - \tau)]\,(e^{-t/\tau} - e^{-t/\tau_0})$$
$$-R'qR\tau_s / [(\tau - \tau_s)(\tau_0 - \tau_s)]\,(e^{-t/\tau_s} - e^{-t/\tau_0}) \quad ...(5)$$

The anode waveform generated by the light emission profile of Figure 1 is now analysed. First, in **figure 5(a)** we consider the current waveform $I(t) = \Sigma\, i(\tau_n)$ where $n = 0$ to 100. The amplitude of $i(t)$ is allowed to vary in accordance with the SER of **figure 4(b)**. Note the ragged appearance of the pulse; the excessive gap in arrival times after about 80 ns, in the particular example given in **figure 1**, causes the output signal to drop to zero. It is clear

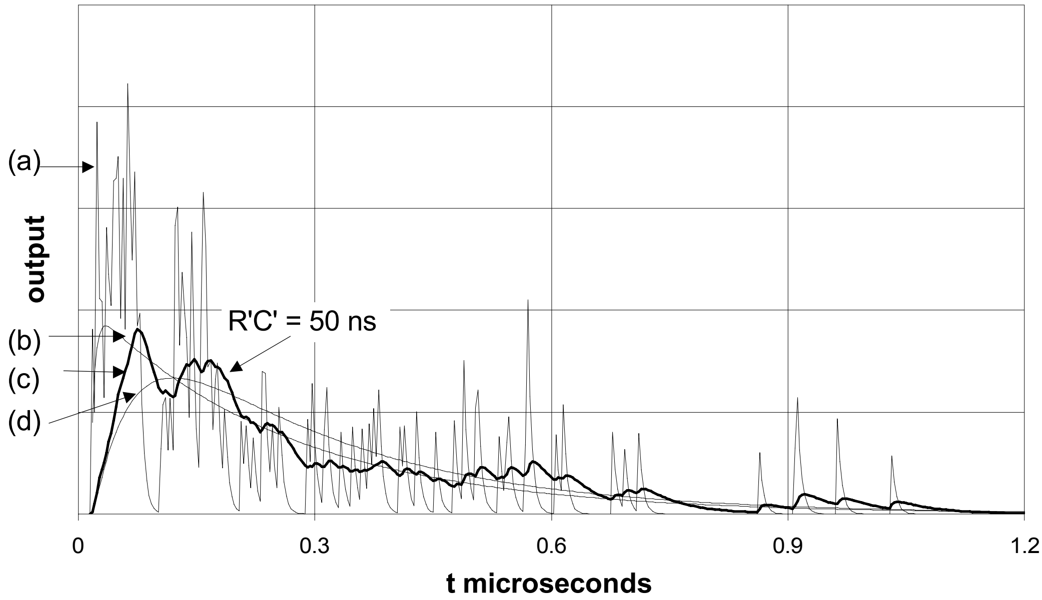

figure 5 a simulation with $R = 100$, $\tau = 250\ ns$, $\tau_s = 5\ ns$, $\tau_0 = 50\ ns$ $NF = 1.17$ and $\varepsilon_{ph} = 5\ ns$. Note the area under all curves is the same.

that if discrimination were attempted on this waveform, at a threshold of say two units on the ordinate, then multiple triggering would result. **Figure 5**(b) refers to (4) and it is the average profile followed by events of type (a). (c) refers to (5) where R'C' has been taken as 50 ns while (d) is the average profile followed by (c).

5 discriminator considerations

The effect of pmt jitter overules the prediction that timing based on the detection of the first photon $(Q = 1)$ will always lead to optimal timing (see **figure 3**) We can take advantage of this to get better timing at the higher Q values while overcoming the possibility of multiple triggering, as observed in **figure 5**. A discriminator based on the constant fraction (CF) technique [4] is preferred for experimental work because it avoids the problem of walk. An inverted fraction of the pulse is added to a delayed version of the pulse itself making the time of zero-crossing walk-free, as illustrated in **figure 6**.

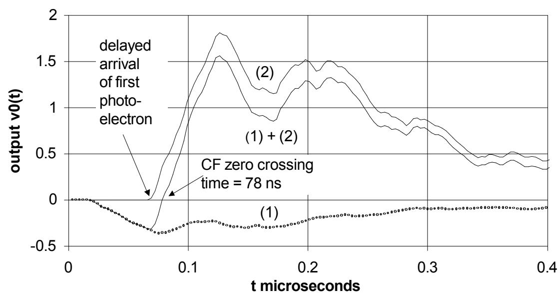

figure 6 applying the CF technique to the waveform of **figure 5**(c). (2) is the main signal delayed by 50 ns; (1) is an attenuated version of (1) without delay; (1)+(2) is the sum of these two signals.

The distribution for zero-crossing times is shown in **figure 7** for two hundred simulations. The sigma of the distribution is degraded directly by the noise factor NF and pmt jitter is responsible for the early arrival times.

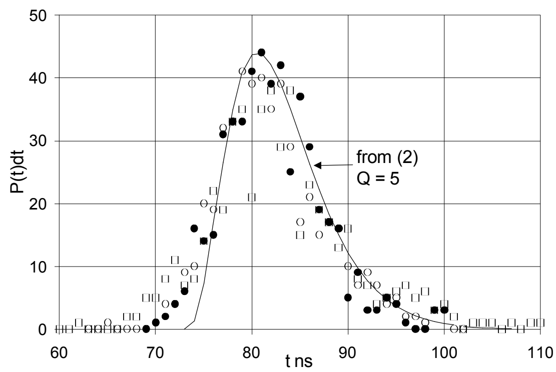

figure 7 CF timing distributions based on 20% and 50 ns delay. ● noiseless gain $(NF = 1)$; ○ $NF = 1.17$; □ $NF = 1.414$. The solid line is equation (2) with $Q = 5$.

6 conclusions

- fast timing with slow scintillators is possible if R/τ is sufficiently large
- although the scintillator decay time is much larger than the pmt jitter, pmt jitter is important at low Q values
- a poor SER degrades timing under all conditions and directly as the noise factor NF
- smoothing is necessary to prevent multiple triggering
- with a constant fraction discriminator, limited smoothing does not degrade performance.
- always resort to experiment with regard to smoothing, threshold, delay and trigger fraction

Important pmt properties are: high QE, good collection efficiency, good SER and low jitter as always.

7 references

[1] R. F. Post and L.I. Shiff. Phys. Rev. 80 (1950) 1113

[2] E. Gatti and V. Svelto Nucl. Instr.and Meth. 43 (1966) 248

[3] G. Ranucci. Nucl. Instr. and Meth. A 335(1993) 121

[4] D.A. Gedcke and W.J. McDonald Nucl. Instr. and Meth. 58 (1968) 253

talk to us about your application or choose a product from our literature:

photomultipliers, voltage dividers, signal processing modules, housings and power supplies

ET Enterprises Limited
45 Riverside Way
Uxbridge UB8 2YF
United Kingdom
tel: +44 (0) 1895 200880
fax: +44 (0) 1895 270873
e-mail: sales@et-enterprises.com
web site: www.et-enterprises.com

ADIT Electron Tubes
300 Crane Street
Sweetwater TX 79556 USA
tel: (325) 235 1418
toll free: (800) 521 8382
fax: (325) 235 2872
e-mail: sales@electrontubes.com
web site: www.electrontubes.com

choose accessories for this pmt on our website

an ISO 9001 registered company

ET Enterprises electron tubes

DS_ R/P098 Issue 3 (18/01/11)